

See discussions, stats, and author profiles for this publication at: <https://www.researchgate.net/publication/263961090>

# Kinetic Aspect on Gelation Mechanism of Tetra-PEG Hydrogel

ARTICLE in *MACROMOLECULES* · MAY 2014

Impact Factor: 5.8 · DOI: 10.1021/ma500662j

CITATIONS

4

READS

54

5 AUTHORS, INCLUDING:



**Kengo Nishi**

Georg-August-Universität Göttingen

15 PUBLICATIONS 79 CITATIONS

SEE PROFILE



**Kenta Fujii**

Yamaguchi University

83 PUBLICATIONS 1,757 CITATIONS

SEE PROFILE



**Takamasa Sakai**

The University of Tokyo

93 PUBLICATIONS 1,537 CITATIONS

SEE PROFILE



**Mitsuhiro Shibayama**

The University of Tokyo

317 PUBLICATIONS 8,701 CITATIONS

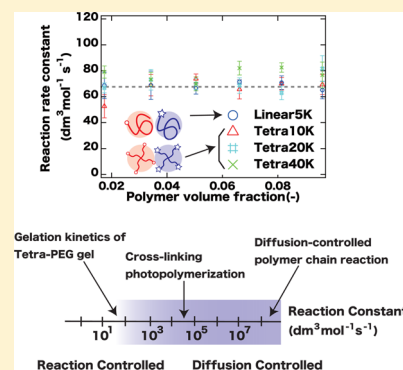
SEE PROFILE

## Kinetic Aspect on Gelation Mechanism of Tetra-PEG Hydrogel

Kengo Nishi,<sup>†</sup> Kenta Fujii,<sup>\*,†,⊥</sup> Yukiteru Katsumoto,<sup>‡</sup> Takamasa Sakai,<sup>§</sup> and Mitsuhiro Shibayama<sup>\*,†</sup><sup>†</sup>Institute for Solid State Physics, The University of Tokyo, 5-1-5 Kashiwanoha, Kashiwa, Chiba 277-8581, Japan<sup>‡</sup>Department of Chemistry, Graduate School of Science, Hiroshima University, 1-3-1 Kagamiyama, Higashihiroshima, Hiroshima 739-8526, Japan<sup>§</sup>Department of Bioengineering, School of Engineering, The University of Tokyo, 7-3-1 Hongo, Bunkyo-ku, Tokyo 113-8656, Japan

## S Supporting Information

**ABSTRACT:** We carried out a kinetic study on the gelation reaction of AB-type cross-end coupling of two tetra-arm poly(ethylene glycol) (Tetra-PEG) prepolymers having amine (Tetra-PEG-NH<sub>2</sub>) and activated ester (Tetra-PEG-NHS) terminal groups by ATR-IR and UV spectroscopies. The reaction rate constant for the gelation of Tetra-PEG,  $k_{\text{gel}}$ , was determined in aqueous solutions with varying both prepolymer volume fraction,  $\phi$ , and molecular weight,  $M_w$ , of the prepolymers. It was clearly found that the value of  $k_{\text{gel}}$  is independent of both  $\phi$  and  $M_w$ , and is comparable to that of the corresponding linear-PEG system. The  $k_{\text{gel}}$  value is obtained to be around 70 dm<sup>3</sup> mol<sup>-1</sup> s<sup>-1</sup>, which is much smaller than the reaction rates of typical diffusion-controlled reaction (e.g., 10<sup>8</sup>–10<sup>9</sup> dm<sup>3</sup> mol<sup>-1</sup> s<sup>-1</sup>) and of cross-linking photopolymerization (10<sup>4</sup>–10<sup>5</sup> dm<sup>3</sup> mol<sup>-1</sup> s<sup>-1</sup>). From these results, we concluded that the gelation reaction of Tetra-PEG gel is not diffusion-limited but reaction-limited process, i.e., the diffusion motion is much faster than the reaction rate. It is thus expected that Tetra-PEG prepolymer chains can diffuse in the solution during gelation process, leading to homogeneity and high-strength of Tetra-PEG gel. These discussions imply that, in order to achieve high-efficient and homogeneous gel, it is necessary to choose reaction groups so as to undergo reaction-limited reaction.



## ■ INTRODUCTION

Gels are defined as three-dimensional polymer networks swollen in solvent. Because of their high retention capacity of solvents, gels are utilized as super absorbent, contact lenses, drug reservoirs, etc. However, industrial applications of gels are still limited because of their low mechanical strength, which result from inhomogeneity created during the cross-linking process. One of the most popular approaches for removing inhomogeneity is an “end-cross-linking” method, which forms a polymer network from AB-type polycondensation of telechelic prepolymers and multifunctional cross-linkers.<sup>1</sup> Because of simplicity of its network structure, mechanical,<sup>2,3</sup> structural,<sup>4–8</sup> and simulational<sup>9–12</sup> studies were conducted on this type of polymer network. However, from these studies, it is found that this network still contains inhomogeneities such as spatial concentration fluctuation, connectivity, and topological defects.<sup>13</sup>

Sakai et al. developed a novel class of hydrogels by “cross-end coupling” of two types of tetra-arm poly(ethylene glycol) (PEG) units that have mutually reactive amine (Tetra-PEG-NH<sub>2</sub>) and activated ester (Tetra-PEG-NHS) terminal groups, respectively (Figure 1a).<sup>14</sup> From SANS measurements on Tetra-PEG gel, it was found that upturns in low- $q$  region ( $q < 0.01$  Å<sup>-1</sup>) are weak, suggesting that Tetra-PEG gels have a near-ideal network.<sup>15,16</sup> Here,  $q$  denotes the magnitude of the scattering vector. Because of its homogeneity, Tetra-PEG gel has several advantages such as high mechanical strength and

toughness. For example, the breaking strength is remarkably high (of the order of a few to tens MPa), being comparable to those of native articular cartilage (approximately 6–10 MPa).<sup>14</sup>

One question may arise why Tetra-PEG gel is so homogeneous. This question is essential and important in order to answer necessary conditions for creating homogeneous networks. In order to answer this question, we focus on the gelation kinetics. In most of gelling systems, such as cross-linking photopolymerizations,<sup>17–26</sup> the gelation kinetics is diffusion controlled, i.e., the reaction kinetics is determined by the diffusion of reactants, and the relationship between diffusion of polymers and gelation kinetics have been extensively studied.<sup>17–34</sup> In those works, the collision rate may change with time as a result of changes in cluster sizes and diffusion of polymers. Hence, multifunctional monomer polymerizations exhibited complex features including autoacceleration and autodeceleration,<sup>27–30</sup> limiting double bond conversion,<sup>27,31–33</sup> and polymerization-rate dependent kinetics.<sup>27,34</sup> On the other hand, in the case of gelation kinetics of Tetra-PEG gel,<sup>35</sup> we pointed out that the gelation kinetics of Tetra-PEG gel undergoes as a simple second-order reaction and  $k_{\text{gel}}$  shows a linear relationship against reciprocal temperature. However, the relationship between diffusion of polymers and

Received: April 1, 2014

Revised: May 7, 2014

Published: May 14, 2014

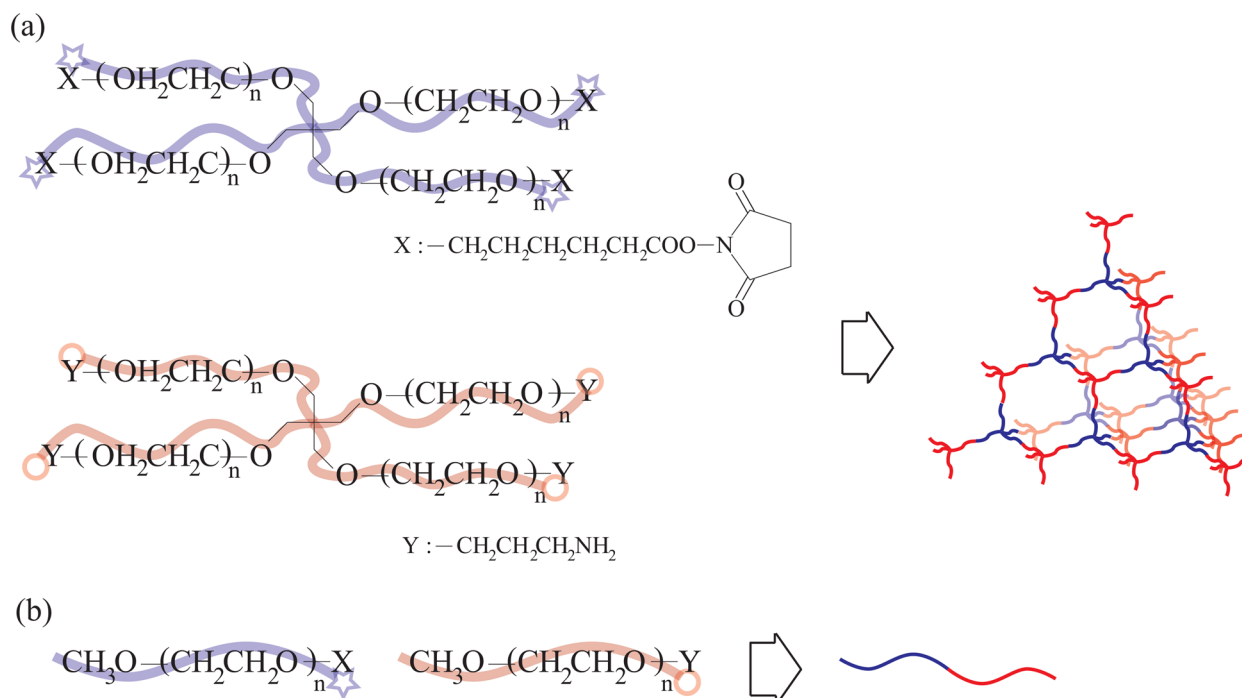


**Figure 1.** Schematic schemes for reactions of (a) Tetra-PEG gel system and (b) linear PEG system.

the gelation kinetics has been unsolved in the previous work, and details of gelation mechanism and the reason why Tetra-PEG gel is so homogeneous are unclear up to now.

In this study, we investigate the relationship between diffusion of polymers and the gelation kinetics of Tetra-PEG gel. It is well-known that the self-diffusion coefficient of linear and star polymer,  $D$ , is strongly dependent on the volume fraction ( $\phi$ ) and the molecular weight ( $M_w$ ) in the semidilute solution.<sup>36–40</sup> In order to elucidate the relationship between diffusion of polymers and reaction kinetics of Tetra-PEG gels, we investigate  $\phi$  and  $M_w$  dependence of the gelation kinetics by IR-ATR and UV spectroscopies. We also examine the kinetics of linear PEG system (Figure 1(b)) for comparison. On the basis of these experiments, we discuss a detailed gelation mechanism and the reason why the gelation kinetics proceeds successfully to form Tetra-PEG gel with high mechanical strength and toughness.

## EXPERIMENTAL SECTION

**Materials.** Tetraamine-terminated PEG (Tetra-PEG-NH<sub>2</sub>; TAPEG) and tetra-NHS-terminated PEG (Tetra-PEG-NHS; TNPEG) prepolymers were purchased from Nippon Oil and Fat Co. The molecular weights,  $M_w$ s of both Tetra-PEG-NH<sub>2</sub> and Tetra-PEG-NHS were matched with each other ( $M_w = 10, 20$ , and  $40 \text{ kg mol}^{-1}$ ). The polydispersities of polymers were narrow ( $M_w/M_n < 1.1$ ) as reported in our previous work.<sup>42</sup> Monofunctional amine-terminated linear PEG (Linear-PEG-NH<sub>2</sub>) and NHS-terminated linear PEG (Linear-PEG-NHS) were also purchased from Nippon Oil and Fat Co. The  $M_w$ s of both Linear-PEGs were matched with each other as  $M_w = 5 \text{ kg mol}^{-1}$ . From this point forward, the Tetra-PEG gels prepared from these prepolymers with  $M_w = 10, 20$ , and  $40 \text{ kg mol}^{-1}$  are named Tetra10K, Tetra20K, and Tetra40K, respectively, and that from Linear-PEG is named Linear5K.

**IR Spectroscopy.** IR measurements with attenuated total reflection (ATR) technique were carried out to obtain quantitative spectra for polymer solutions. Details about ATR-IR measurements are described in ref 35. Constant amounts of Tetra-PEG-NH<sub>2</sub> ( $M_w = 10 \text{ kg mol}^{-1}$ ; volume fraction of polymer,  $\phi = 0.034\text{--}0.15$ ) and Tetra-

PEG-NHS ( $M_w = 10 \text{ kg mol}^{-1}$ ;  $\phi = 0.034\text{--}0.15$ ) were dissolved in phosphate-buffered D<sub>2</sub>O (0.2 M, pH 7). Here, the polymer volume fraction ( $\phi$ ) was calculated from polymer concentration ( $c$ ,  $\text{g mL}^{-1}$ ) as follows:  $\phi = w_{\text{PEG}}/(w_{\text{PEG}} + w_{\text{water}}) = (c/\rho_{\text{PEG}})/\{1 + (c/\rho_{\text{PEG}})\}$ ,<sup>14</sup> where  $w_{\text{PEG}}$ ,  $w_{\text{water}}$  and  $\rho_{\text{PEG}}$  are the weight of PEG in solution, the weight of water in solution, and the density of PEG ( $1.129 \text{ g mL}^{-1}$ ), respectively. The two solutions thus obtained were mixed in a 50 mL Falcon tube for 30 s at 20 °C, and poured into the ATR cell. The ATR cell was maintained at 20 °C throughout the entire experiment. In order to deconvolute IR spectra and extract single bands, we conducted fitting analysis on IR spectra by using the sum of pseudo-Voigt functions. Fitting analysis is discussed in detail in our previous work.<sup>35</sup>

**UV Spectroscopy.** UV spectra were recorded on JASCO UV-vis spectrophotometer V-630, Nihon-bunko, Japan. The quartz cell (thickness: 0.2 cm) was kept at 20 °C throughout the entire experiment. As previously reported,<sup>35</sup> the terminal NHS in PEG-NHS is hydrolyzed during the gelation process. Thus, we evaluate the hydrolysis kinetics at first. A given amount of PEG-NHS ( $5 \text{ kg mol}^{-1}$  Linear-PEG, 15 mg;  $10 \text{ kg mol}^{-1}$  Tetra-PEG, 7.5 mg;  $20 \text{ kg mol}^{-1}$  Tetra-PEG, 15 mg;  $40 \text{ kg mol}^{-1}$  Tetra-PEG, 30 mg) was dissolved in 3.0 mL of water including 0.2 M phosphate buffer (pH 7.0) at 20 °C, and the solution was added into an quartz cell just after sample preparation. The measurement time (total) was about 40000 s corresponding to the end of the hydrolysis, and the time interval was 120 s at each spectrum. In coupling reaction system, aqueous PEG-NH<sub>2</sub> and PEG-NHS solutions with same polymer concentration ( $\phi$ : 0.034–0.12) and 0.2 M phosphate buffer (pH 7) were prepared and then they were mixed in a 50 mL Falcon tube for 30 s at 20 °C, followed by pouring into the cell. Detail procedure of the measurements is the same with above hydrolysis system.

## RESULTS AND DISCUSSION

**Reaction Kinetics.** The chemical reactions of Tetra-PEG gel system involve (i) aminolysis between the amine group within TAPEG and activated ester (*N*-hydroxysuccinimide) (NHS) ester group within TNPEG, (ii) hydrolysis of the activated ester group within TNPEG, and (iii) protonation equilibrium of the terminal NH<sub>2</sub> group of TAPEG. As for protonation equilibrium, the equilibrium constant  $K_a$  is defined

as  $K_a = [-\text{NH}_2][\text{H}^+]/[-\text{NH}_3^+]$ . More details about the reactions are described in our previous work.<sup>35</sup>

In the gelation system, only neutral amine group,  $-\text{NH}_2$  reacts with the activated ester group to form amide bond, whereas protonated amine group,  $-\text{NH}_3^+$  does not react due to absence of an unshared electron pair within terminal  $\text{NH}_3^+$ . Therefore, the reaction rate equation for the gelation is described as follows.

$$-\text{d}[-\text{NH}_2]_{\text{total}}/\text{d}t = k_{\text{gel}}[-\text{NH}_2][-\text{NHS}] = k_{\text{gel}}f \quad (1)$$

$$[-\text{NH}_2]_{\text{total}}[-\text{NHS}]$$

$$-\text{d}[-\text{NHS}]/\text{d}t = k_{\text{gel}}f[-\text{NH}_2]_{\text{total}}[-\text{NHS}] + k_{\text{hyd}}[-\text{NHS}] \quad (2)$$

Here,  $[-\text{NH}_2]_{\text{total}}$  is defined as the total concentration ( $\text{mol dm}^{-3}$ ) of amine group within TAPEG, i.e.,  $[-\text{NH}_2]_{\text{total}} = [-\text{NH}_2] + [-\text{NH}_3^+]$ . In addition,  $k_{\text{hyd}}$ ,  $k_{\text{gel}}$ , and  $f$  denote the rate constant for the hydrolysis, that of the gelation, and the fraction of neutral amine to total amine, i.e.,  $f = [-\text{NH}_2]/[-\text{NH}_2]_{\text{total}} = K_a/(K_a + [\text{H}^+])$ , respectively. Here,  $f$  can be calculated from  $K_a$  and pH in the solution. The  $K_a$  value was separately determined by potentiometric titration for TAPEG solution to be  $10^{-9.27} \text{ mol dm}^{-3}$  from our previous work.<sup>41</sup> On the other hand, though pH was mainly controlled by using phosphate buffer, pH was slightly varied depending on  $[-\text{NH}_2]_{\text{total}}$  in solution. Therefore, in this work, the dependence of  $[-\text{NH}_2]_{\text{total}}$  on pH was measured using a IS-FET electrode, which is described in detail in the Supporting Information (Figure S1). On the basis of the above rate equations, we evaluate  $k_{\text{gel}}$  in the following section.

**IR Measurement on the Gelation Kinetics.** Figure 2 shows the time variation of the concentration of the dissociated

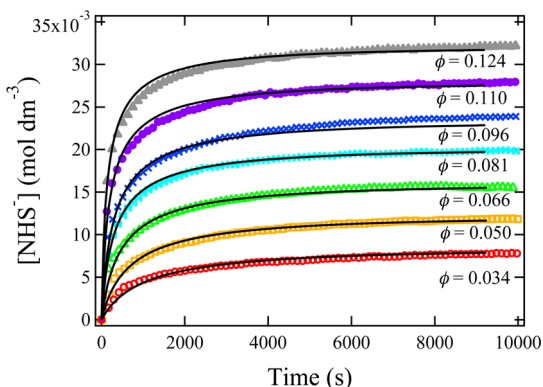


**Figure 2.** Kinetic trace obtained for the gelation at  $1646 \text{ cm}^{-1}$  (C–O stretching vibration of dissociated NHS) as a function of time. The solid lines are fitting results with eq 1 and 2

NHS ion,  $[\text{NHS}^-]$  during the gelation reaction with various polymer concentrations (Tetra10K). The symbols show the observed data, and the solid lines show the fitting results of eqs 1 and 2. Details of evaluation procedure of  $[\text{NHS}^-]$  are described in the Supporting Information (Figure S2). Here,  $k_{\text{hyd}}$  is fixed to the value ( $7.28 \times 10^{-5} \text{ s}^{-1}$ ), which is obtained from the hydrolysis analysis as discussed in our previous work.<sup>35</sup> The observed data are well represented with the theoretical lines in this time range examined here to give the rate constant,  $k_{\text{gel}}$ . Figure 3 shows the obtained  $k_{\text{gel}}$ s plotted against polymer

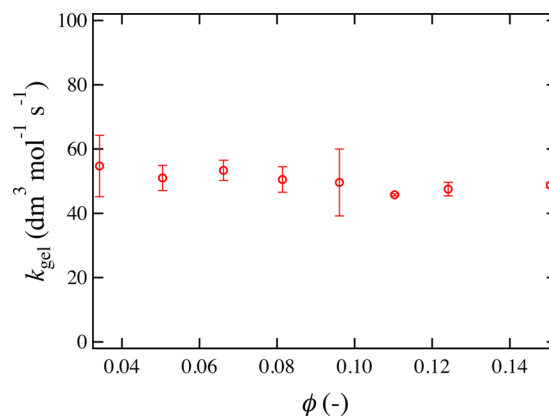


**Figure 3.**  $k_{\text{gel}}$  plotted against polymer concentration  $\phi$ .

concentration  $\phi$ . As can be seen in Figure 3, the  $k_{\text{gel}}$  values are almost constant regardless of polymer concentration, and are almost the same as those reported for the aminolysis of anisoyl–NHS and *n*-butylamine in aqueous dioxane, 20% (v/v) in the literature,  $50.9 \text{ dm}^3 \text{ mol}^{-1} \text{ s}^{-1}$ .<sup>43</sup> From the facts that (1)  $k_{\text{gel}}$  is not dependent on  $\phi$  and (2)  $k_{\text{gel}}$  is almost the same as those of the aminolysis in a low molecular system in this concentration range, we can point out that the gelation reaction of Tetra-PEG gel is considered to be not diffusion-limited but reaction-limited. In order to investigate the gelation mechanism for further details, it is necessary to examine the effect of polymer dynamics on the reaction kinetics by using higher-molecular-weight prepolymer. However, when we use high-molecular-weight prepolymers, the concentrations of terminal NHS and dissociated NHS are low. In that case, because the peak intensity is weak, it is difficult to evaluate the concentration of the dissociated NHS from IR measurement. Thus, we conducted UV measurements on the gelation kinetics in the following sections.

**UV Measurement on the Hydrolysis Kinetics of Tetra-PEG-NHS.** Figure 4a shows the UV spectra for the hydrolysis kinetics of Linear-PEG-NHS ( $M_w = 5 \text{ kg mol}^{-1}$ ,  $\phi = 0.0044$ ). It has been already established in the previous work<sup>44</sup> that the dissociated NHS, i.e.,  $[\text{NHS}^-]$  in water system shows the absorbance at around 260 nm, whereas it is not for Tetra-PEG-NHS before hydrolysis or gelation. As can be seen in Figure 4a, the peak intensity observed at 260 nm gradually increased as the gelation reaction proceeds, indicating that the hydrolysis reaction undergoes in the aqueous solution. Similar to the IR results, the dissociated  $[\text{NHS}^-]$  is calculated as follows:

$$[\text{NHS}^-](t) = \frac{[-\text{NHS}]_0}{A_{260}(\infty)} A_{260}(t) \quad (3)$$

Here,  $[\text{NHS}^-](t)$ ,  $[-\text{NHS}]_0$ ,  $A_{260}(\infty)$ , and  $A_{260}(t)$  denotes the concentration of the dissociated NHS ion at time  $t$ , the initial concentration of the terminal NHS, the IR intensity at 260  $\text{cm}^{-1}$  at the end of reaction, and at time  $t$ , respectively. Figure 4b shows the kinetic trace of  $[\text{NHS}^-]$  in four PEG-NHS systems (Linear5K, Tetra10K, Tetra20K, and Tetra40K). We thus estimated the hydrolysis rate constant,  $k_{\text{hyd}}$  by least-squares fitting analysis on the basis of the following rate equation:  $-\text{d}[-\text{NHS}]/\text{d}t = \text{d}[\text{NHS}^-]/\text{d}t = k_{\text{hyd}}[-\text{NHS}]$ . The observed variation was well represented with the fitting curve (solid line) for all the systems. The  $k_{\text{hyd}}$  values for Tetra-PEG-NHS of  $M_w = 10, 20$ , and  $40 \text{ kg mol}^{-1}$  could be estimated to be  $2.1 \times 10^{-4}$ ,  $1.8 \times 10^{-4}$ , and  $1.9 \times 10^{-4} \text{ s}^{-1}$ , respectively, and that for



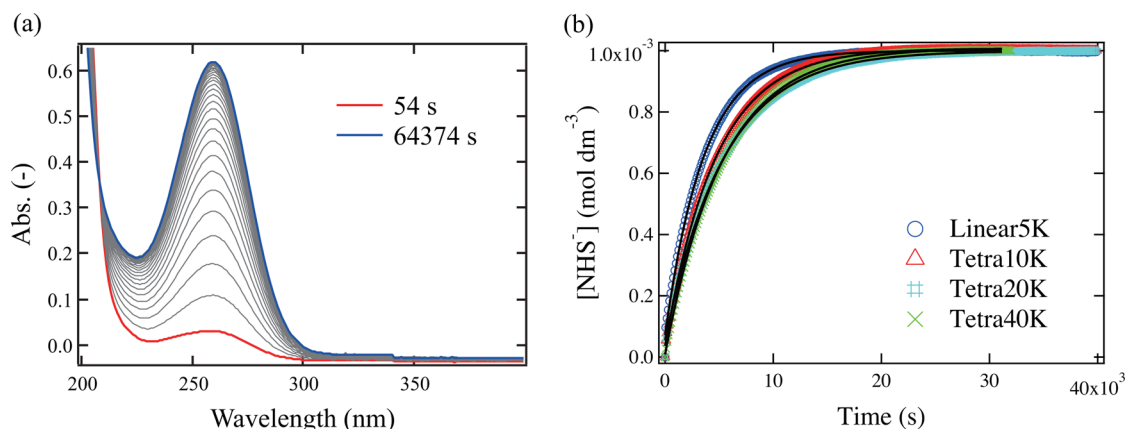


**Figure 4.** (a) Time dependence of UV spectra for the hydrolysis of linear PEG ( $\phi = 0.044$ ) in solution containing 0.2 M phosphate buffer (pH 7.0). The time interval of data shown in this figure is 1200 s. (b) Kinetic trace obtained for the hydrolysis of terminated NHS at 260 nm as a function of time. The solid lines are fitting results with eq 2 and  $k_{\text{gel}} = 0$ .

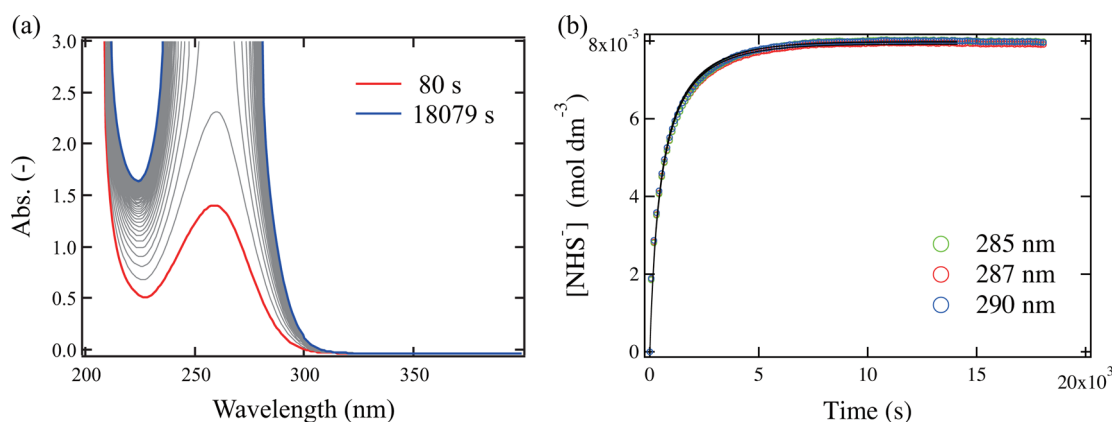


**Figure 5.** (a) Time dependence of UV spectra for the gelation of 20K Tetra-PEG prepolymers (TNPEG,  $\phi = 0.066$ ; TAPEG,  $\phi = 0.066$ ) in solution containing 0.2 M phosphate buffer (pH 7.0). The time interval of data shown in this figure is 120 s. (b) Kinetic trace obtained for the gelation at 285, 287, and 290 nm as a function of time. The solid lines are fitting results with eqs 1 and 2

LinearPEG-NHS to be  $2.8 \times 10^{-4} \text{ s}^{-1}$ . To evaluate the gelation rate constant,  $k_{\text{gel}}$  in this work, these values were used as the fixed parameters in the following fitting analysis.

**UV Measurement on the Gelation Kinetics of Tetra-PEG Gel.** In addition, a mixed solution of LinearPEG-NH<sub>2</sub> and LinearPEG-NHS is named Linear5K. Figure 5a shows the time dependence of UV spectra for the coupling kinetics of Tetra20K ( $\phi = 0.066$ ). As shown in Figure 5a, the peak intensity at 260 nm was completely saturated over the reaction time 320 s. Therefore, we evaluated the dissociated NHS<sup>−</sup> concentration, [NHS<sup>−</sup>] from the absorbance at 285, 287, and 290 nm, resulting in a similar kinetic trace among them (see Figure 5b). Here, the evaluation procedure of [NHS<sup>−</sup>] from absorption spectra is the same as the previous section. The solid lines in Figure 5b show the theoretical curve obtained from fitting analysis using eqs 1 and 2, which is in good agreement with the observed data from the initiation to nearly completion of reaction. The same procedure was applied to Tetra10K, Tetra40K, and Linear5K with various polymer concentrations.

Figure 6 shows concentration dependences of the kinetic trace of [NHS<sup>−</sup>] for (a) Linear5K, (b) Tetra10K, (c) Tetra20K, and (d) Tetra40K systems. The  $k_{\text{hyd}}$  is fixed to the value determined from the hydrolysis analysis in the previous section. Here, note that the gelation point was estimated to be  $p = 0.46$

for tetrafunctional networks from our previous work of degradation test.<sup>45</sup> The observed data (symbols) are well represented with the fitting one (solid line) for all the systems, in the gelation entire time-range from the initiation to nearly completion of reaction.

The gelation rate constant,  $k_{\text{gel}}$  was successfully estimated for all the systems, which is shown in Figure 7. It is rather surprising that the  $k_{\text{gel}}$  values obtained here are almost constant within experimental error regardless of polymer volume fraction,  $\phi$ , and prepolymer molecular weight,  $M_w$ , and their  $k_{\text{gel}}$  values for Tetra-PEG gel are close enough to those for linearPEG system (Linear5K). It is well-known that the linear and star polymer can diffuse even in a semidilute solution and the self-diffusion coefficient of polymer chains,  $D$ , is dependent on the volume fraction ( $\phi$ ) and the molecular weight ( $M_w$ ).<sup>36–40</sup> If the reaction is diffusion-limited,  $k_{\text{gel}}$  should vary with  $M_w$  and  $\phi$ . In addition, we can point out that these  $k_{\text{gel}}$  values correspond to the aminolysis of a low-molecular weight system<sup>43</sup> such as  $50.9 \text{ dm}^3 \text{ mol}^{-1} \text{ s}^{-1}$ , and are much smaller than other diffusion limited systems. For example, the diffusion-controlled quenching rate constant between two end-labeled polystyrenes in solutions is in the range of  $10^8$ – $10^9 \text{ dm}^3 \text{ mol}^{-1} \text{ s}^{-1}$ , which depends on polymerization degree and polymer concentration.<sup>46–50</sup> For another example, the rate constants for cross-linking photopolymerization of multi(metha)acrylates

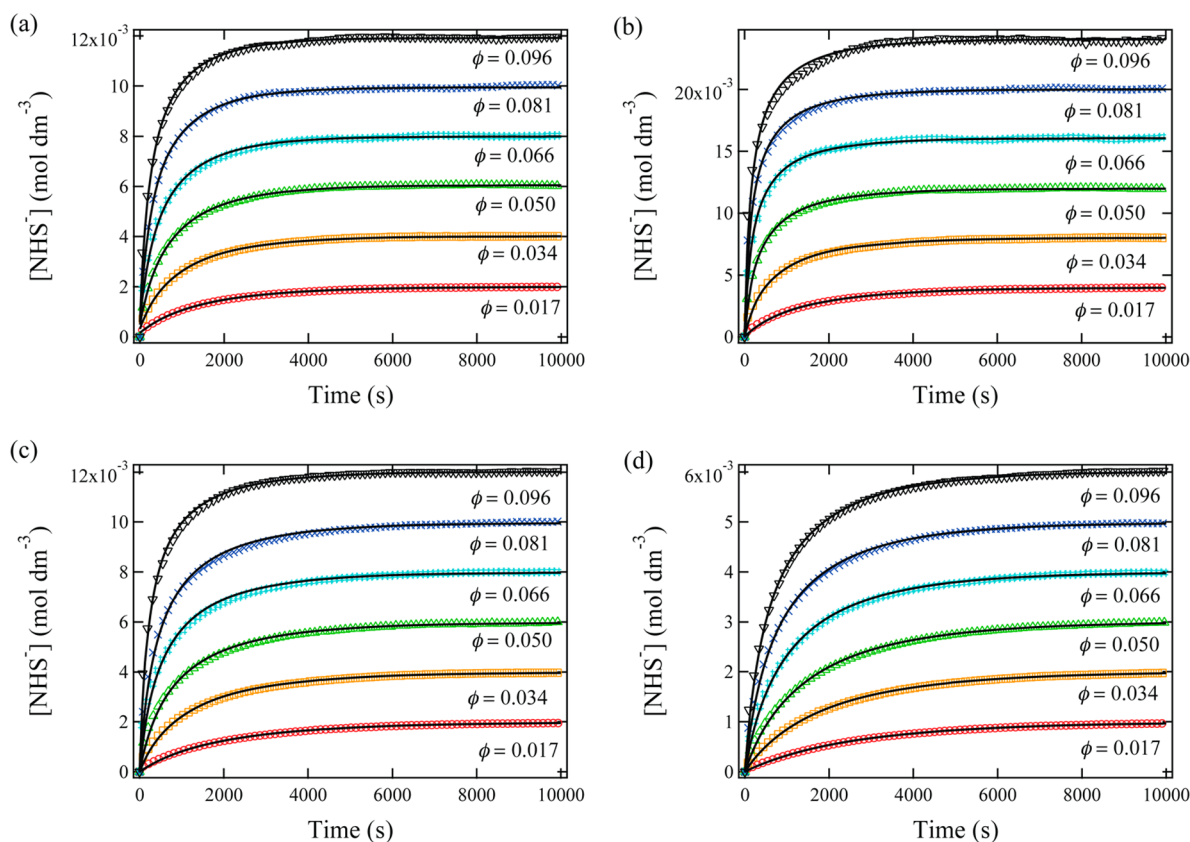


**Figure 6.** Kinetic trace obtained for the gelation of (a) Linear5K, (b) Tetra10K, (c) Tetra20K, and (d) Tetra40K. The solid lines are fitting results with eqs 1 and 2

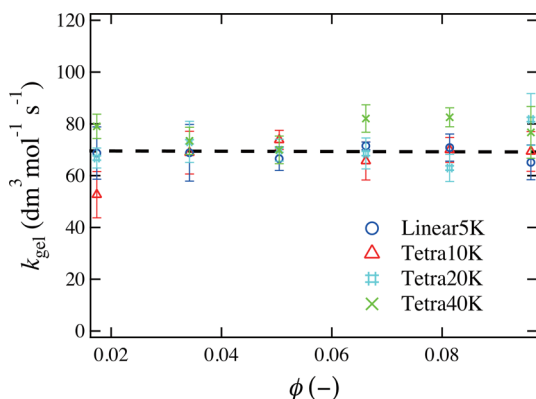


**Figure 7.**  $k_{\text{gel}}$  plotted against polymer concentration  $\phi$  for Linear5K, Tetra10K, Tetra20K, and Tetra40K.

and epoxy-amine monomers are in the order of  $10^4$ – $10^5$   $\text{dm}^3 \text{mol}^{-1} \text{s}^{-1}$ , which depend on the chain-lengths of the monomer and cross-linker concentration.<sup>17–34</sup> In this work, on the other hand, we quantitatively evaluated the rate constants of Tetra-PEG gel to be around  $70 \text{ dm}^3 \text{mol}^{-1} \text{s}^{-1}$ , which does not depend on the prepolymer molecular weight and concentration. Note that the value of  $k_{\text{gel}}$  is  $10^7$ – $10^8$  times smaller than that of diffusion-controlled reaction of polymer solutions irrespective of the difference in the arm number. We thus conclude here that the gelation kinetics of Tetra-PEG gel is the reaction-limited mechanism not diffusion-limited one. That is, the reaction rate of the amide bond formation is much slower than the collision rate of the terminal NHS and amine groups. A comparison of the relative values of  $k_{\text{gel}}$  is shown in Figure 8.

We have already reported that Tetra-PEG gel has an excellent mechanical property due to a homogeneous polymer network.<sup>14,51</sup> In addition, in our previous work, we measured temperature dependence of the gelation kinetics of Tetra-PEG gel and found that (i) the gelation kinetics of Tetra-PEG gel undergoes as a simple second-order reaction and (ii) the estimated rate constant,  $k_{\text{gel}}$  shows a linear relationship against reciprocal temperature.<sup>35</sup> However, we could not discuss a detailed gelation mechanism and the reason why polymer network was homogeneously formed in Tetra-PEG system in the previous work.<sup>35</sup> In this study, we revealed, from the  $\phi$  and  $M_w$  dependence of gelation kinetics, that the gelation reaction of Tetra-PEG gel is reaction-limited process. On the basis of this experimental finding, we propose the detailed mechanism of gelation process and one of the reasons why polymer network is homogeneously formed in Tetra-PEG system as follows.

We depict a schematic picture for the reaction process of the diffusion-limited and the reaction-limited cases for AB type cross-end coupling reaction in Figure 9. First, we focus on the diffusion-limited case. The state after sufficient mixing is shown in Figure 9b. A and B must be uniformly dispersed with time averaging. However, when we focus on a specific time, A is not necessarily located next to B and A could be located next to A at a certain rate even after sufficient mixing. Thus, there must be some spots where the concentration of A (or B) is higher than the average. This situation is depicted in Figure 9b. In the case of the diffusion-limited reaction, the reaction rate of A and B is much faster than the diffusion motion. Therefore, A and B react just after encountering, and the local concentration of A and B at a specific time may be suddenly frozen before A and B

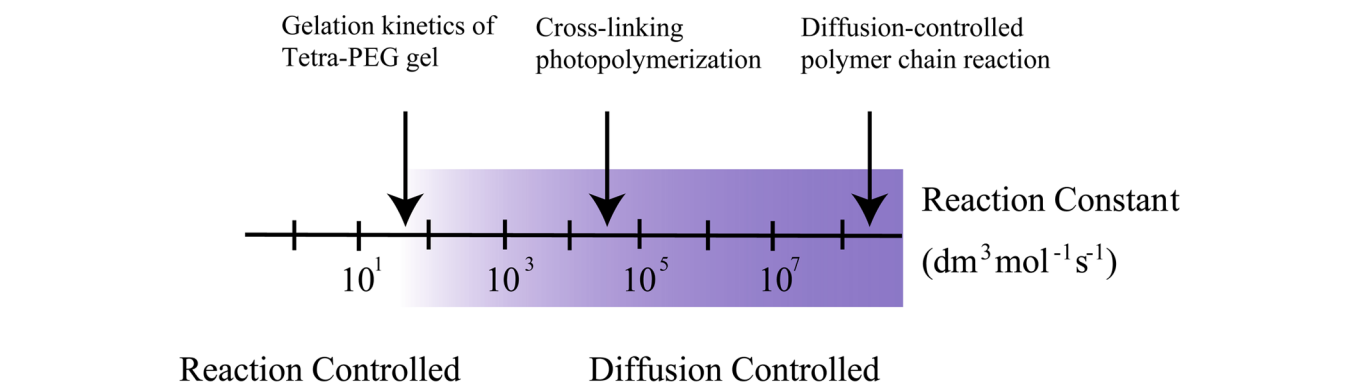


**Figure 8.** Comparison of reaction rate constants of Tetra-PEG gel, cross-linking photopolymerization, and diffusion-controlled polymer chain reaction.

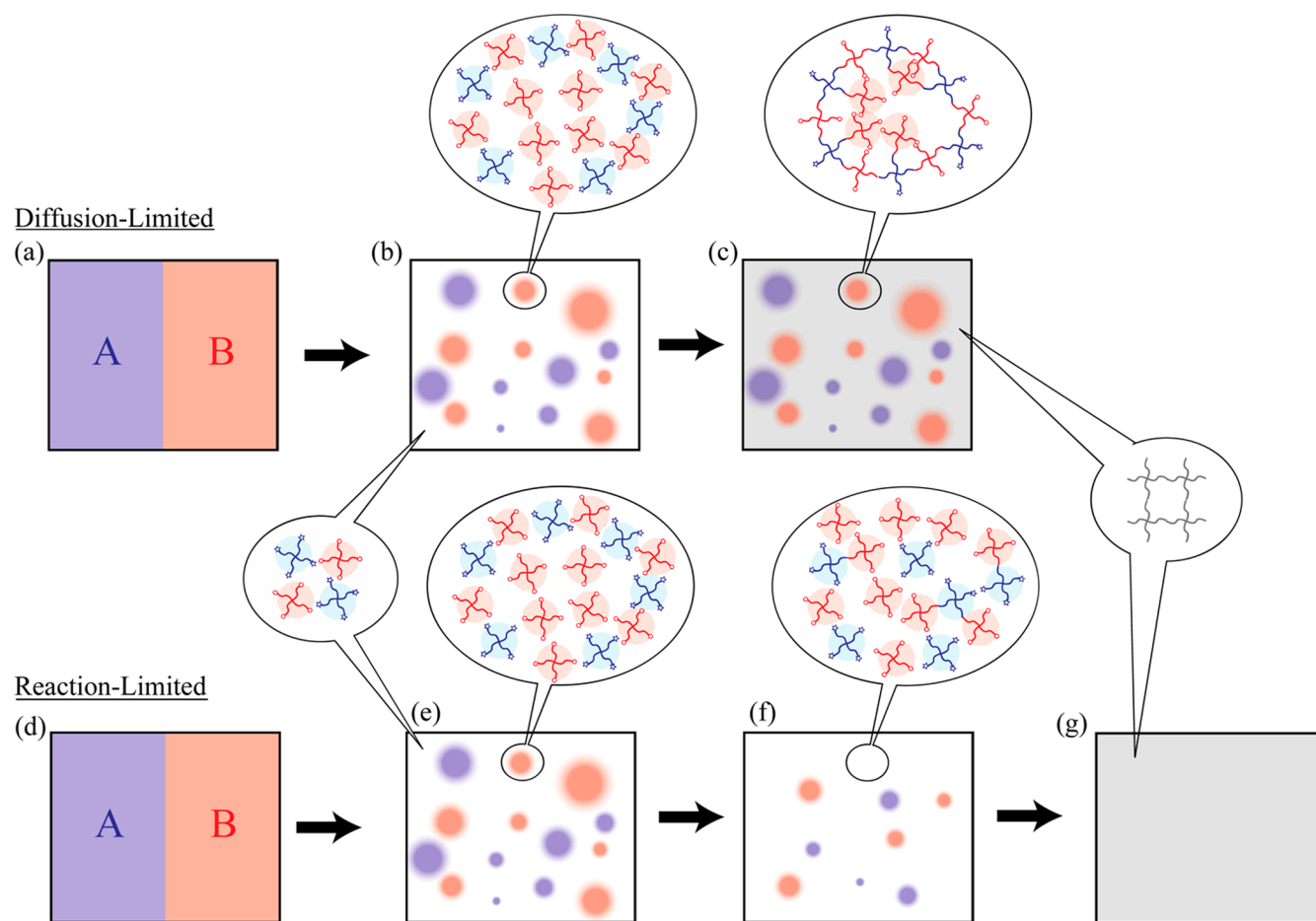


**Figure 9.** Schematic picture of AB type cross-end coupling reaction in the case of diffusion-limited gelation and reaction-limited gelation: (a, d) Premixing state; (b, e) state after sufficient mixing; (f) early stage of reaction; (c, g) the final state of gelation reaction.

diffuse, leading to frozen inhomogeneities (Figure 9c). On the other hand, in the case of the reaction-limited reaction, which is the case of Tetra-PEG gel, the reaction rate of A and B is much slower than the diffusion motion. Even if A is next to B, the encountered pairs are often separated without bond formation. Therefore, A and B prepolymers could sufficiently diffuse during the gelation process and the gelation reaction proceeds efficiently and uniformly as depicted in Figure 9, parts f and g. These discussions imply that, in order to achieve high-efficient and homogeneous gel, it is necessary to choose reaction groups so as to become the reaction-limited.

Lastly, it should be noted that not only diffusion controlled reaction may cause formation of inhomogeneity. In general, there exist several types of inhomogeneities in gels, such as spatial concentration fluctuations, connectivity defects, and topological defects.<sup>13</sup> Spatial concentration fluctuations are inhomogeneity of molecular weight between cross-links and polymer density. Connectivity defects are nonaccomplishment of full conversion of gelation reaction due to topological limitation. Third, topological defects represent defects of network, such as loops and entanglements. Because of end-linking of symmetric 4-arm star polymers, inhomogeneity of

molecular weight between cross-links and topological defects are greatly suppressed in Tetra-PEG gel system. Especially, suppression of loop formation was revealed by simulation<sup>52,53</sup> and experimental<sup>54</sup> studies. Simulation works expect that loop formation kinetics depends on the polymer concentration and there is a difference in reaction rate constant between monofunctional polymer reaction and loop formation reaction.<sup>52,53</sup> However, as shown in Figure 7, the reaction rate constant of linear-PEG system corresponds to that of Tetra-PEG system, which might indicate that loop formation scarcely occurs. The decrease of loop formation was also confirmed from low-field multiple-quantum NMR.<sup>54</sup> In addition to this, the inhomogeneity of polymer density and the connectivity defects are reduced due to uniform progression of gelation reaction because gelation reaction of Tetra-PEG gel is reaction-controlled. Owing to these multiple causes, Tetra-PEG gel possesses a near-ideal network.

## CONCLUSION

The gelation mechanism of Tetra-PEG gel was investigated by IR and UV measurements. It was found that the reaction rate constant of gelation kinetics of Tetra-PEG gelation is independent of polymer concentration and the prepolymer molecular weight. In addition, the reaction rate is comparable to that of linear-PEG systems, and corresponds to the aminolysis of a low molecular system. The value of  $k_{\text{gel}}$  for Tetra-PEG gel is obtained to be around  $70 \text{ dm}^3 \text{ mol}^{-1} \text{ s}^{-1}$ , which is much smaller than the reaction rate of typical diffusion-controlled reaction (e.g.,  $10^8$ – $10^9 \text{ dm}^3 \text{ mol}^{-1} \text{ s}^{-1}$ ). These results clearly indicate that the gelation reaction of Tetra-PEG gel is not diffusion-limited but reaction-limited. It is concluded that the reaction-limited reaction is one of the keys to fabricate homogeneous polymer networks.

## ASSOCIATED CONTENT

### Supporting Information

Fraction of un-ionized amine as a function of total amine concentration, equations used in the calculations, and IR spectra and discussion. This material is available free of charge via the Internet at <http://pubs.acs.org>.

## AUTHOR INFORMATION

### Corresponding Authors

\*E-mail: k-fujii@yamaguchi-u.ac.jp (K.F.).

\*E-mail: sibayama@issp.u-tokyo.ac.jp (M.S.).

### Present Address

<sup>†</sup>Graduate School of Science and Engineering, Yamaguchi University, 2-16-1 Tokiwadai, Ube, Yamaguchi 755-8611, Japan.

### Notes

The authors declare no competing financial interest.

## ACKNOWLEDGMENTS

This work has been financially supported by Grant-in-Aids for Scientific Research from the Ministry of Education, Culture, Sports, Science, and Technology (No. 13J00449 to K. N., No. 24750066 to K. F., No. 23700555 to T.S., Nos. 22245018 and to 25248037 to M.S.). K.N. acknowledges the support from Research Fellowship for Young Scientists of the Japan Society for the Promotion of Science.

## REFERENCES

- (1) Hild, G. *Prog. Polym. Sci.* **1998**, *23*, 1019–1149.
- (2) Michalke, W.; Lang, M.; Kreitmeier, S.; Goeritz, D. *J. Chem. Phys.* **2002**, *117* (13), 6300–6307.
- (3) Valles, E. M.; Macosko, C. W. *Macromolecules* **1979**, *12* (4), 673–679.
- (4) Takahashi, H.; Shibayama, M.; Fujisawa, H.; Nomura, S. *Macromolecules* **1995**, *28*, 8824–8828.
- (5) Takahashi, H.; Shibayama, M.; Hashimoto, M.; Nomura, S. *Macromolecules* **1995**, *28*, 5547–5553.
- (6) Mendes, E.; Girard, B.; Picot, C.; Buzier, M.; Boue, F.; Bastide, J. *Macromolecules* **1993**, *26*, 6873.
- (7) Shibayama, M.; H, T.; Yamaguchi, H.; Sakurai, S.; Nomura, S. *Polymer* **1994**, *35*, 2944–2951.
- (8) Shibayama, M.; Takahashi, H.; Nomura, S. *Macromolecules* **1995**, *28*, 6860–6864.
- (9) Duering, E. D.; Kremer, K.; Grest, G. S. *J. Chem. Phys.* **1994**, *101*, 8169–8192.
- (10) Gilra, N.; Cohen, C.; Panagiotopoulos, A. Z. *J. Chem. Phys.* **2000**, *112*, 6910–6916.
- (11) Michalke, W.; Kreitmeier, S.; Lang, M.; Buchner, A.; Goritz, D. *Comput. Theor. Polym. Sci.* **2001**, *11*, 459–466.
- (12) Svaneborg, C.; Grest, G. S.; Everaers, R. *Polymer* **2005**, *46*, 4283–4295.
- (13) Shibayama, M.; Norisuye, T. *Bull. Chem. Soc. Jpn.* **2002**, *75*, 641–659.
- (14) Sakai, T.; Matsunaga, T.; Yamamoto, Y.; Ito, C.; Yoshida, R.; Suzuki, S.; Sasaki, N.; Shibayama, M.; Chung, U. *Macromolecules* **2008**, *41* (14), 5379–5384.
- (15) Matsunaga, T.; Sakai, T.; Akagi, Y.; Chung, U.; Shibayama, M. *Macromolecules* **2009**, *42* (4), 1344–1351.
- (16) Matsunaga, T.; Sakai, T.; Akagi, Y.; Chung, U.; Shibayama, M. *Macromolecules* **2009**, *42* (16), 6245–6252.
- (17) Anseth, K. S.; Kline, L. M.; Walker, T. A.; Anderson, K. J.; Bowman, C. N. *Macromolecules* **1995**, *28*, 2491–2499.
- (18) Li, W.-H.; Hamielec, A. E.; Crowe, C. M. *Polymer* **1989**, *30*, 1513–1517.
- (19) Li, W.-H.; Hamielec, A. E.; Crowe, C. M. *Polymer* **1989**, *30*, 1518–1523.
- (20) Zhu, S.; Tian, Y.; Hamielec, A. E.; Eaton, D. R. *Polymer* **1990**, *31*, 154–159.
- (21) Scranton, A. B.; Bowman, C. N.; Klier, J.; Peppas, N. A. *Polymer* **1992**, *33*, 1683–1689.
- (22) Young, J. S.; Bowman, C. N. *Macromolecules* **1999**, *32*, 6073–6081.
- (23) Cook, W. D. *J. Polym. Sci. A Polym. chem.* **1993**, *31*, 1053–1067.
- (24) Berchtold, K. A.; Bowman, C. N. *RadTech Eur. 99 Conf. Proc.* **1999**, 767.
- (25) Anseth, K. S.; Wang, C. M.; Bowman, C. N. *Macromolecules* **1994**, *27*, 650–655.
- (26) Schulz, G. V. *Z. Phys. Chem. (Munich)* **1956**, *8*.
- (27) Kloosterboer, J. G. *Adv. Polym. Sci.* **1988**, *84*, 1–61.
- (28) Miyazaki, K.; Horibe, T. *J. Biomed. Mater. Res.* **1988**, *22* (11), 1011–1022.
- (29) Allen, P.; Simon, G.; Williams, D.; Williams, E. *Macromolecules* **1989**, *22*, 809–816.
- (30) Cook, W. D. *Polymer* **1992**, *33*, 600–609.
- (31) Simon, G.; Allen, P.; Bennett, D.; Williams, D.; Williams, E. *Macromolecules* **1989**, *22* (2), 3555–3561.
- (32) Allen, P.; Bennett, D.; Hagias, S.; Hounslow, A.; Ross, G.; Simon, G.; Williams, D.; Williams, E. *Eur. Polym. J.* **1989**, *25*, 785–789.
- (33) Kloosterboer, J.; Lijten, G.; Boots, H. *Makromol. Chem., Macromol. Symp.* **1989**, *24*, 223–230.
- (34) Bowman, C. N.; Peppas, N. A. *Macromolecules* **1991**, *24*, 1914–1920.
- (35) Nishi, K.; Fujii, K.; Chijiishi, M.; Katsumoto, Y.; Chung, U.; Sakai, T.; Shibayama, M. *Macromolecules* **2012**, *45* (2), 1031–1036.
- (36) Martin, J. E. *Macromolecules* **1984**, *17*, 1279–1283.



- (37) de Gennes, P. G. *Scaling Concepts in Polymer Physics*. Cornell University: Ithaca, NY, 1979.
- (38) von Meerwall, E.; Tomich, D. H.; Grigsby, J.; Pennisi, R. W.; Fetters, L. J.; Hadjichrisidis, N. *Macromolecules* **1983**, *16*, 1715–1722.
- (39) von Meerwall, E.; Tomich, D. H.; Hadjichrisidis, N.; Fetters, L. J. *Macromolecules* **1982**, *15*, 1157–1163.
- (40) Xuexin, C.; Zhongde, X.; von Meerwall, E.; Seung, N.; Hadjichrisidis, N.; Fetters, L. J. *Macromolecules* **1984**, *17*, 1343–1348.
- (41) Kurakazu, M.; Katashima, T.; Chijiishi, M.; Nishi, K.; Akagi, Y.; Matsunaga, T.; Shibayama, M.; Chung, U.; Sakai, T. *Macromolecules* **2010**, *43* (8), 3935–3940.
- (42) Akagi, Y.; Gong, J. P.; Chung, U. I.; Sakai, T. *Macromolecules* **2013**, *46* (3), 1035–1040.
- (43) Cline, G. W.; Hanna, S. B. *J. Org. Chem.* **1988**, *53*, 3583–3586.
- (44) Miron, T.; Wikchek, M. *Anal. Biochem.* **1982**, *126*, 433–435.
- (45) Li, X.; Tsutsui, Y.; Matsunaga, T.; Shibayama, M.; Chung, U.; Sakai, T. *Macromolecules* **2011**, *44*, 3567–3571.
- (46) Mita, I.; Horie, K.; Takeda, M. *Macromolecules* **1981**, *14*, 1428–1433.
- (47) Friedman, B.; O'Shaughnessy, B. *Macromolecules* **1993**, *26*, 5726–5739.
- (48) Friedman, B.; O'Shaughnessy, B. *Europhys. Lett.* **1993**, *23* (9), 667–672.
- (49) Friedman, B.; O'Shaughnessy, B. *Macromolecules* **1993**, *26* (4888–4898), 4888.
- (50) O'Shaughnessy, B. *Macromolecules* **1994**, *27*, 3875–3884.
- (51) Shibayama, M. *Soft Matter* **2012**, *8*, 8030–8038.
- (52) Lang, M.; Schwenke, K.; Sommer, J.-U. *Macromolecules* **2012**, *45*, 4886–4895.
- (53) Schwenke, K.; Lang, M.; Sommer, J.-U. *Macromolecules* **2011**, *44* (23), 9464–9472.
- (54) Lange, F.; Schwenke, K.; Kurakazu, M.; Akagi, Y.; Chung, U.; Lang, M.; Sommer, J.-U.; Sakai, T.; Saalwachter, K. *Macromolecules* **2011**, *44*, 9666–9674.